Macromolecules
ARTICLE

Macromolecules **2009**, *42*, 5843–5850 **5843**
DOI: 10.1021/ma900438u

Stationary Electric Birefringence of Flexible Polyelectrolyte Solutions: Experimental Evidence of Different Counterion Polarization Mechanisms

Hernán A. Ritacco,*,‡ David Kurlat,† Ramón G. Rubio,‡ Francisco Ortega,‡ and Dominique Langevin§

†*Facultad de Ingeniería, Universidad de Buenos Aires. Argentina,* ‡*Depto. Química-Física I. Facultad de Cs. Químicas, Universidad Complutense de Madrid, Madrid. Spain, and* §*Laboratoire de Physiques des Solides. Université de Paris-XI Sud. Orsay. France*

Received February 26, 2009; Revised Manuscript Received July 1, 2009

ABSTRACT: Transient electric birefringence (TEB) measurements on aqueous solutions of flexible polyelectrolytes (in pure water, with added salt and with oppositely charged surfactants) are presented. The results evidence the different polarization mechanism of free and condensed counterions. Free counterions polarize perpendicular to the main polymer axis and give a negative contribution to the birefringence; condensed counterions polarize parallel to the main polymer axis and give a positive contribution. We present a simple model that allows to explain the change in sign of the birefringence when polymer, salt and surfactant concentrations are varied, according to which polarization mechanism prevails. From the model we can estimate the fraction of free counterions obtaining values which are close to the values calculated with Manning theory. We demonstrate the interest of TEB technique in the study of polyelectrolyte/surfactant systems.

1. Introduction

When a polyelectrolyte is dissolved in water, an atmosphere of counterions surrounds the polyelectrolyte chain.[1] Current models for polyelectrolyte solutions are generally based on counterion condensation, an idea first introduced by Imai and Onishi[2] and Oosawa[3] and developed later by Manning.[4] Manning's important contributions to the model were recognized by the scientific community and the model is today known as Manning condensation theory. The basic idea underlying this model is that when the charge density on a linear polyelectrolyte chain exceeds a critical value (such that the electrical potential along the chain reaches the value kT/e, k being the Boltzmann constant, T the absolute temperature, and e the electron charge), the exceeding charge must be neutralized by counterions. Part of the counterions then condenses onto the polymer chain, close to the charged group, so that the chain potential does not exceeds kT/e.

Let us consider the case of monovalent counterions and introduce the Bjerrum length, $l_b = e^2/(\varepsilon kT)$; l_b is the distance at which the electrostatic interaction equals the thermal energy, ε being the dielectric constant. Counterion condensation will occur when $b/f < l_b$, b being the monomer length and $1/f$ the number of monomers separating charged groups (f is the nominal charge per monomer). The fraction of counterions that condenses, $(1 - \varphi)$ will be such that the final effective charge density corresponds to the Bjerrum length. In the frame of this model, the fraction of free counterions, φ can be obtained by $\varphi = b/(l_b f)$.

The counterion atmosphere plays an important role in the polarization mechanism of polyelectrolytes in solution and controls the electric properties of the solutions as well as the interactions between polyelectrolytes and other charged entities, such as surfactants or nanoparticles.

A variety of theoretical models have been proposed to describe the origin of the induced dipole moment of polyelectrolytes.[5] Some of them assume that only bound counterions contribute to the polarizability.[6] Today, there is experimental evidence that both type of counterions, free and condensed, play a role in the polarization mechanism.[7] Hayakawa and co-workers[8] have carried out experiments of frequency domain electric birefringence spectroscopy (FEB) on sodium polystyrene sulfonate (NaPSS) solutions and concluded that condensed counterions move along the polyelectrolyte chain and that free (or loosely bound) counterions move perpendicularly to the chain. The contributions to the birefringence of each polarization mechanism have opposite signs. We present here transient electric birefringence (TEB) experiments on flexible polyelectrolyte solutions in pure water and mixed with salts and oppositely charged surfactants. Our objectives are to understand first, the change of the birefringence sign when polyelectrolyte concentration increases, which was considered an anomaly,[9] and second, the effect of surfactants. Polyelectrolyte- surfactant systems became an intensive area of research in the recent years and have numerous practical applications in cosmetics, paints and coatings, detergents and pharmaceuticals.[10] When the surfactant bears a charge opposite to that of the polyelectrolyte, it replaces the original counterion and eventually forms polyelectrolyte−surfactant complexes. The aggregation process is in general a cooperative phenomenon that occurs above a given surfactant concentration called the critical aggregation concentration (CAC). Here we present TEB results that show how the sign of the electrically induced birefringence of a polyelectrolyte aqueous solution can be changed by eliminating one of the two possible counterion polarization mechanism. This can be done in particular by adding an opposite charged surfactant which, above the CAC, condenses onto the polymer backbone. The results give information on both polarization mechanisms and on the complexation of polyelectrolytes and surfactants. We present a simple model to estimate the electric birefringence when polymer, salt and surfactant concentrations are varied.

*Corresponding author. E-mail: ritacco@quim.ucm.es.

Published on Web 07/14/2009

Table 1. Polyelectrolyte Characteristics

PAMPS	N^a	M_{mon} (g·mol^{-1})	f	Nb^b (nm)	$c_{ov}{}^c$/ (mM)	A^d/monomers	L^e (nm)
P10	4100	100.9	0.1	1025	0.12	10	376
P20	3600	116.8	0.2	900	0.55	5	491
P25	3400	124.75	0.25	850	0.044	4	527
P50	2830	164.5	0.5	657	0.59	~3	480

[a] Polymerization degree. [b] Contour length, $b = 0.25$ nm is the monomer size. [c] Overlap concentration (in monomers) calculated with eq 6. [d] Effective distance between charges expressed in monomers calculated from Manning criterion. [e] Actual extended size of polymer chains calculated with eq 2.

2. Materials and Methods

2.1. Transient Electric Birefringence. Under the action of an external electric field (E) a sample, originally isotropic, becomes birefringent (the refractive index becomes anisotropic). This phenomenon is called Kerr effect, and it is generally attributed to the orientation of the molecules under the action of the electric field. The experimental setup for measuring Kerr effect used here was described elsewhere.[11] The birefringence is defined as $\Delta n = n_{\parallel} - n_{\perp}$ where $n_{\parallel}$ and $n_{\perp}$ are the refractive index in the directions parallel and perpendicular to the applied electric field respectively. As long as the field is applied, the birefringence increases and tends to a stationary value, Δn_0. This value can become positive or negative depending on the relative values of $n_{\parallel}$ and $n_{\perp}$. In most liquids, and for low electric field intensities, the induced birefringence is a linear function of E^2,

$$\Delta n^0 = BE^2\lambda \tag{1}$$

λ being the wavelength of the light source used and B, a proportionality constant called the Kerr constant. Because we are dealing with solutions of polyelectrolytes in water, in all the results presented here we have subtracted the contribution of water to obtain the pure polymer contribution. The transient regime of the induced birefringence, after E is applied or removed, can be analyzed as well. However, here we will deal only with the stationary value of the birefringence, Δn^0, and Kerr constants. The birefringence relaxation results will be discussed in a future paper.

2.2. Chemicals. The polyelectrolytes used in this work are anionic statistical copolymers of neutral acrylamide monomers and charged acrylamido methyl propane sulfonate monomers (PAMPS). Polyelectrolytes with different ratio f of the number of sulfonated monomers to the total number of monomers were used. We will call P50, P25, P20, and P10 the polymers with $f = 0.5$, 0.25, 0.2, and 0.1 respectively. The polyelectrolytes were synthesized by SNF Floerger (France); their characteristics are summarized in Table 1. All polyelectrolytes are very soluble in water which is a good solvent. The salt used is NaCl from Sigma-Aldrich (purity >99.9%). The cationic surfactant used is dodecyl trimethyl ammonium bromide (DTAB), purchased from Sigma-Aldrich and purified twice by recrystallization (2 g of DTAB: 10 mL of ethyl acetate: 1 mL of ethyl alcohol). The solutions were prepared in Millipore Milli-Q water. All measurements were carried out at 298 ± 0.1 K.

3. Results and Discussion

3.1. Theoretical background. Let us consider a solution of a flexible polyelectrolyte with concentration c (expressed in number of monomers per unit volume).[12] Let us call N the total number of monomers in a chain, if A is the average number of monomers separating adjacent charges, including any effect of counterion condensation, the total effective charge on a chain will be N/A. At a short scale, the chain is coiled and forms electrostatic blobs, and its total length, in good solvent condition, is given by:

$$L = Nb\left(\frac{l_b}{bA^2}\right)^{2/7} \tag{2}$$

Here, $b = 0.25$ nm, $l_b = 0.7$ nm. The quantity $[l_b/(bA^2)]^{2/7}$ is therefore of order $^1/_2$, and the coiling due to electrostatic blobs is minor: $L \sim Nb/2 \sim 500$ nm (see Table 1). Additional coiling comes from the fact that the length of the polymer is longer than the persistence length l_p. The end to end distance of the chain is given by

$$R = l_p\left(\frac{L}{l_p}\right)^{3/5} \tag{3}$$

The persistence length contains an intrinsic contribution l_p^0 and an electrostatic contribution, l_p^e.

$$l_p = l_p^0 + l_p^e \tag{4}$$

For intrinsically rigid chains, the electrostatic contribution to the persistence length is given by the Odijk−Skolnick−Fixman (OSF) theory,[13] $l_p^e = \frac{l_b}{4\kappa^2(bA)^2}$, where κ is the inverse Debye length: $\kappa = (4\pi l_b fc)^{1/2}$. The OSF model can be applied to flexible and strongly charged polyelectrolytes[14] for which the electrostatic contribution to the total persistence length is dominat. For intrinsically flexible and weakly charged chains and in the absence of screening, Khokhlov and Khachaturian (KK)[15] were the first to derive that $l_p^e = \frac{1}{4\kappa^2 D_e}$. They have arrived to this expression by applying the OSF theory to a string of crumpled blobs, i.e., by considering the blobs as new effective monomers, been D_e the blob size and where the intrinsic persistence length, l_p^0 (eq 4) is equal to the blob size. This result was rederived later in the framework of variational approach.[16]

Here, the main contribution to l_p is the electrostatic contribution. When the polymer concentration is sufficiently small, less than 0.1 mM, the amount of counterions dissociated from the polyion is very high and l_p is large, so that the polymer remains in an extended configuration: $L \sim l_p \sim R$. The polymers will then overlap easily and the overlap concentration, c_{ov} for salt free polyelectrolyte solutions, can be estimated as,

$$c_{ov} = \frac{N}{L^3} \tag{5}$$

With $N \sim 4000$ and $L \sim 500$ nm, we find $c_{ov} \sim 0.1$ mM (~10 mg·L^{-1}). Because of all experiments for salt-free solutions were performed at concentrations above c_{ov}, we will restrict for now our discussion to the semidilute regime. The major feature of a semidilute solution is the existence of a correlation length ξ,[17] given in the case of polyelectrolytes by

$$\xi = L\left(\frac{c}{c_{ov}}\right)^{-1/2} \tag{6}$$

Correlations are lost after a distance ξ, so the extension of the chain decreases above c_{ov}. The number of monomers in the correlation volume being $g \approx c\xi^3$, the end-to-end distance R is given by

$$R = \xi\left(\frac{N}{g}\right)^{1/2} = L\left(\frac{c}{c_{ov}}\right)^{-1/4} \tag{7}$$

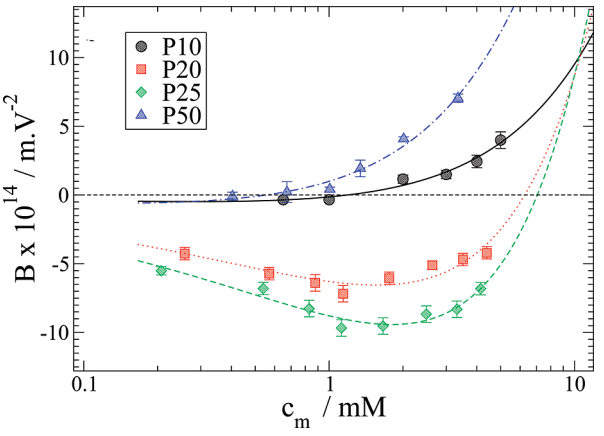

Figure 1. Kerr constant as a function of monomers concentration. Points are experimental results, and lines fit curves using eq 15.

3.2. TEB Results. Salt-Free Solutions. In Figure 1 we show the Kerr constant B as a function of concentration for all PAMPS polymers. The birefringence is negative for all PAMPS at very low concentrations. We can see clearly a minimum for P20 and P25. This minimum could exist also for P50 and P10 but at very low concentrations. For P10 and P50 there is a change of the sign of the birefringence from negative to positive values. For P20 and P25, Δn^0, and consequently B, is always negative in the entire range of concentrations explored: 6×10^{-5} mM $< c < 1.2 \times 10^{-3}$ mM (25 to 500 mg·L^{-1}). This behavior of the birefringence as polyelectrolyte concentration increases was also observed in a fully charged polyelectrolyte, NaPSS, by Kramer et al. (see Figure 2 in ref 9). The birefringence of PSS solutions evolves from zero to negative values, reaches a minimum and then increases to positives values as polymer concentration increases ($0.001 < c < 1$ g/L), which is similar to PAMPS behavior (see Figure 1). At higher PSS concentrations ($c >$ 1 g/L) Kramer et al. found that the birefringence passes through a maximum and falls again to negative values as c increases even more. We did not reach those high concentrations and we did not see this last behavior.

A complete and rigorous analysis of the Kerr constant is difficult for simple molecules but almost impossible for macromolecules and particularly for flexible polyelectrolytes. We will use here the following simplified analysis. The induced birefringence per molecule can be expressed as the product of two factors:[18]

$$\Delta n \propto \Delta\alpha^0 \Phi(t) \tag{8}$$

The first one, $\Delta\alpha^0$, is the intrinsic anisotropy of the optical molecular polarizability: $\Delta\alpha^0 = \alpha_\parallel^0 - \alpha_\perp^0$, with $\alpha_\parallel^0$ and $\alpha_\perp^0$ being the polarizabilities in the directions parallel and perpendicular to the molecule main axes. The second factor in eq 9 is the orientation function, $\Phi(t)$, which reflects the degree of orientation of the molecule in the electric field. The orientation function depends on the interaction energy between permanent and induced molecular dipole moments with the external electric field. As we have mentioned before, getting an explicit and detailed expression for this function is rather complicated for a simple molecule and almost impossible for a macromolecule, especially if the macromolecule is flexible and can change its conformation easily. Here for simplicity, we will adopt a cylindrical rigid geometry for the polyelectrolyte molecule (see Figure 2). The real molecule is made of cylindrical portions of length l_p, which

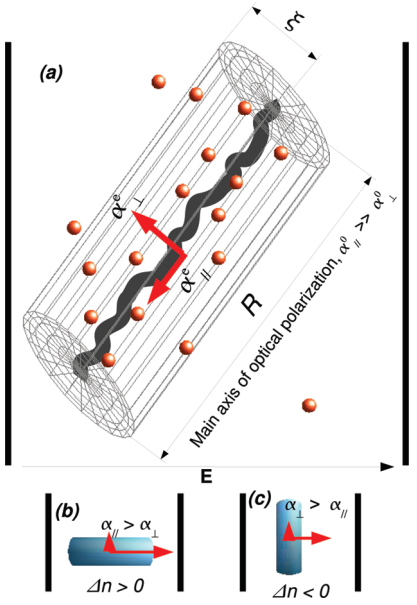

Figure 2. Cylindrical polyelectrolyte in an electric field. (a) Definition of parameters. (b) Main axis of the macromolecule oriented parallel to the applied field, positive birefringence. (c) Main axis of the macromolecule oriented perpendicular to the applied field, negative birefringence.

is however quite large at low polymer concentrations as discussed before. If we assume that the molecule has no permanent dipoles (only induced dipoles) and restrict our analysis to constant and low electric fields (Kerr regime), the orientation function is[18]

$$\Phi = \frac{\Delta\alpha^e E^2}{15kT} \tag{9}$$

where $\Delta\alpha^e$ is the anisotropy of electric polarizability of the molecule which is the difference between electrical polarizabilities $\alpha_\parallel^e$ and $\alpha_\perp^e$ in the directions respectively parallel and perpendicular to the cylinder ($\Delta\alpha^e$ corresponds to the frequency of the applied electric field, whereas $\Delta\alpha^0$ corresponds to the frequency of the optical field, used for the detection). Now, from eqs 1, 8, and 9, we obtain

$$B \approx c\Delta\alpha^0 \frac{\Delta\alpha^e}{15kT} \tag{10}$$

where we have introduced the monomer concentration c. We need now to give an explicit expression for $\Delta\alpha^e$. To do so we assume that our polyelectrolyte chain is a cylinder (Figure 2) of total length R given by eq 7. Following Ito et al.,[8] we will consider that the electric polarizability has contributions only from the condensed counterions polarized parallel to the cylinder and from free counterions polarized perpendicular to the cylinder. The polarization of condensed counterions tends to orientate the main molecular axes parallel to the external electric field whereas free counterions polarization tends to orientate the molecules perpendicular to the field. Note that the sign of the contribution to the birefringence of each polarization mechanism depends on the sign of $\Delta\alpha^0$, we assume that the main optical axis lies on the main polymer backbone and then $\Delta\alpha^0 > 0$. Then, the condensed counterions give a positive contribution to the birefringence and free counterions a negative one. Ito et al. also showed that the α^e are of the order of the mean-square diffusion

Table 2. Fitting Parameters of Eq 14 Corresponding to Figure 1[a]

PAMPS	$a_0/m^4\ V^{-2}$	$a_0/m^2\ V^{-2}$	n
P10	1.36×10^{-37}	1.14×10^{-25}	0.47
P20	4.9×10^{-38}	1.01×10^{-25}	0.51
P25	7.8×10^{-38}	1.51×10^{-25}	0.50
P50	5.96×10^{-38}	3.35×10^{-26}	0.50

[a] They correspond to concentrations c in terms of number of molecules per unit volume.

length, the end to end distance R for $\alpha_{\|}^e$ and the correlation length ξ for $\alpha_{\|}^e$:

$$\alpha_{||}^e = \frac{\langle \mu_{||}{}^2 \rangle}{kT} = \frac{e^2 R^2}{kT}$$

$$\alpha_{\perp}^e = \frac{\langle \mu_{\perp}{}^2 \rangle}{kT} = \frac{e^2 \xi^2}{kT} \tag{11}$$

where ξ and R are given by eqs 6 and 7 respectively. Now, from eqs 10 and 11, we have

$$B \sim c \frac{\Delta\alpha^0}{15kT} \left\{ \frac{(1-\varphi) f e^2 R^2}{kT} - \frac{\varphi f e^2 \xi^2}{kT} \right\} \tag{12}$$

The polarization mechanisms of condensed and free counterions have relaxation frequencies in the range of kilohertz and megahertz, respectively; they are too slow to contribute at optical frequencies.[8] In the absence of a detailed molecular model, we will assume that

$$\Delta\alpha^0 \sim \Delta\alpha_m^0 c^n \tag{13}$$

where $\Delta\alpha_m^0$ is the anisotropy of optical polarizability of monomers. Finally from eqs 12 and 13 with 6 and 7 we obtain the expression for B as a function of monomer concentration c

$$B = a_0 c^{n+1/2} - a_1 c^n$$

$$a_0 = \frac{\Delta\alpha_m^0}{15(kT)^2} (1-\varphi) f e^2 L^2 c_{ov}{}^{1/2}$$

$$a_1 = \frac{\Delta\alpha_m^0}{15(kT)^2} \varphi f e^2 L^2 c_{ov} \tag{14}$$

In Figure 1, the lines are fitting curves using eq 14. The three parameters, a_0, a_1, and n obtained for the four polymers are summarized in table 2. The exponent n is very close to $^1/_2$. If we fix $n = {}^1/_2$ and refit the curves, the parameters a_0 and a_1 are very similar to those in table 2. Note that this simple model predicts the change of sign of the birefringence when polymer concentration changes (see Figure 1). This is considered an anomalous behavior and it was found experimentally in other similar systems.[9] This effect is mainly explained in our simple model (eq 12) by the changes on R and ξ due to the changes on the polymer concentration (eqs 6 and 7).

As said before, P20 and P25 present a minimum in the Kerr constant B as c increases. If we take the derivative of eq 14 to find the position of that minimum, we find the following expression

$$\frac{2(1-\varphi)}{\varphi} = \left(\frac{c_{\min}}{c_{ov}} \right)^{-1/2} \tag{15}$$

For P20 the minimum occurs at $(c_{P20})_{min} \sim 1.3$ mM and for P25 at $(c_{P25})_{min} \sim 1.2$ mM. With these values and eq 15, we calculate the fraction of free counterions $\varphi = 0.92$ and 0.91 for P20 and P25 respectively. For these two polymers, the Manning condensation criterion predicts that $\varphi = 1$ ($b/f > l_b$). There are four possible explanations for this *small* discrepancy: first the model, expressed by eq 12, is incomplete in the sense that it neglects the contribution of electronic polarizability in front of the counterions polarization effect. The main axes of electronic polarizability lies on the main macromolecule axes and then has a positive contribution to the birefringence, this positive contribution, neglected by the model, increases artificially the calculated counterion condensation fraction obtained from it. This effect should be more important for the less charged polyelectrolyte, P10. Second, PAMPS are *statistical* copolymers, meaning that the distances between charged groups can be larger or smaller than the average value $1/f$ (table 1), and some counterions could be condensed in the regions of larger charge density. Third, for flexible polyelectrolytes, the distances between adjacent charges on the polymer chain are reduced due to the bending of chains and as a consequence an increasing of counterion condensation is expected.[19] Fourth, the Manning criterion is valid for isolated chains, and when several chains are present, again the distance between charges can be smaller than $1/f$. In any case, the value of $\varphi \sim 0.92$ found for P20 and P25 is encouraging and gives us a certain confidence in our rather naive model. In the case of P10 and P50, no minimum is visible in Figure 1. We can however use eq 14 to estimate φ for all the polyelectrolytes. We calculate the relation a_0/a_1 and solve for φ to obtain

$$\varphi = \frac{\frac{a_1}{a_0} c_{ov}{}^{-1/2}}{1 + \frac{a_1}{a_0} c_{ov}{}^{-1/2}} \tag{16}$$

Then, from the values of Tables 1 and 2 we calculate $\varphi = 0.74$, 0.93, 0.93, and 0.78 for P10, P20, P25, and P50 respectively. First note that the values found for φ in the case of P20 and P25 are almost the same obtained by using eq 15 and the experimental value for c_{min}. Again φ is lower than one for P10 contrary to expected from the Manning criterion, but closer to one for P20 and P25. In the case of P10 a possible explanation was stated in the previous paragraph: P10 is a very weak charged polyelectrolyte and eq 12 is incomplete in the sense that it neglects the electronic polarization which could be of relative importance in front of the little amount of counterions that can polarize the macromolecule. This neglected contribution to the birefringence is positive and then it increases artificially the calculated counterion condensation from the previous equations. As we said before, this effect is less important for the others PAMPS with higher values of f.

For P50 $\varphi < 1$ and close to the value given by Manning theory, $\varphi = 0.67$. The values obtained in this way are quite robust and do not depend much on N and L: calculations with $N = 4000$ for the four polymers or $L = 500$ nm for all give the same values of φ within 1 or 2%.

If we go ahead and estimate from the expression for a_0 or a_1 (eq 14) the values of $\Delta\alpha_m^0$ for each polyelectrolyte, we find $\Delta\alpha_m^0 = 1.0 \times 10^{-36}$, 1.2×10^{-36}, 6.7×10^{-37}, and $1.54 \times 10^{-37}\ m^3$ for P10, P20, P25, and, P50 respectively. We can now estimate the anisotropy of the optical polarizability of

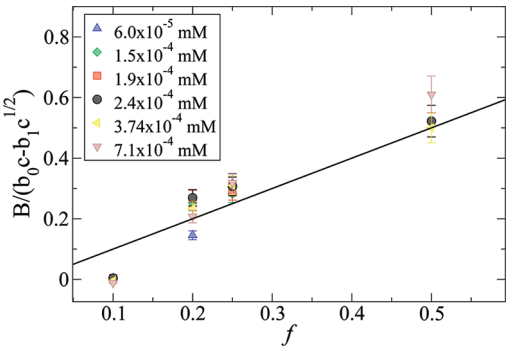

Figure 3. Dependence of electric induced birefringence on the degree of charge on the polyelectrolyte chain. The line corresponds to $B/(b_0c - b_1c^{1/2}) = f$ (see text).

polyelectrolyte molecules as $\Delta\alpha^0 \sim N\alpha_m^0$ obtaining $\Delta\alpha^0 = 4.1 \times 10^{-33}$, 4.32×10^{-33}, 2.3×10^{-33}, and 4.0×10^{-34} m^3 for P10, P20, P25, and P50, respectively. We have then a relation $B/\Delta\alpha^0 \sim 1.5 \times 10^{19}$. These values of the optical anisotropy of the macromolecule are physically realistic, for example for a polyelectrolyte having a poly(*p*-phenylene) backbone, a value of $B/\Delta\alpha^0 \sim 10^{19}$ was found[20] and for PSS a value of $B/\Delta\alpha^0 \sim 9 \times 10^{19}$.[21] Note that the optical anisotropy for P50 is 1 order of magnitude smaller than the others; it may be in this case that some of the symmetry on the distribution of the sulfonate groups on the molecule is responsible for this low optical anisotropy.

Equation 14 also gives the dependence of B on the degree of charge of the polyelectrolyte, f: $B/(b_0c - b_1c^{1/2}) \sim f^m$ where $m = 1$ (if we suppose $\alpha_m{}^0$ independent of φ) and $b_0 = a_0/f$ and $b_1 = a_1/f$. In Figure 3, we show the experimental points and a line for $m = 1$ at six different polymer concentrations. If we fit the experimental points with $B/(b_0c - b_1c^{1/2}) = f^m$ we find $m = 1.06$, 0.98, 0.95, 0.94, 0.98, and 0.92 for polyelectrolyte concentrations of 0.6×10^{-4}, 1.55×10^{-4}, 1.9×10^{-4}, 2.4×10^{-4}, 3.74×10^{-4}, and 7.14×10^{-4} mM respectively. These values are very close to $m = 1$ as the model predicts, and again our simple model seems to give good results.

3.3. TEB Results. Polyelectrolyte−Salt Solutions. In Figure 4, we present results for B as a function of salt concentration, c_s keeping the polymer concentration constant, for all PAMPS and at different polymer concentrations. Because only a small amount of P50 was available to us, only one concentration was studied in this case.

Equation 12 is still valid, but new expressions for ξ and R are needed, in order to take into account the influence of salt. Indeed, the overlap concentration c_{ov} changes as salt concentration increases. The screening length and the end-to-end distance in the presence of salt and in a good solvent are given by[22]

$$\xi = \left(\frac{N}{Lc}\right)^{1/2}\left(1+2A\frac{c_s}{c}\right)^{1/4}$$

$$R = \left(\frac{NL}{c}\right)^{1/4}\left(1+2A\frac{c_s}{c}\right)^{-1/8} \qquad (17)$$

for semidilute solutions and

$$\xi = \left(\frac{N}{Lc}\right)^{1/2}\left(1+2A\frac{c_s}{c}\right)^{-1/2}$$

$$R = \left(\frac{NL^2}{c}\right)^{1/5}\left(1+2A\frac{c_s}{c}\right)^{-1/5} \qquad (18)$$

for dilute solutions, where the concentrations are expressed in number of monomers per unit volume. The overlap concentration is given by[12,22]

$$c_{ov}\left(1+2A\frac{c_s}{c_{ov}}\right)^{-3/2} \approx \frac{N^{-2}}{b^3}\left(\frac{A^2b}{l_b}\right)^{6/7} = \frac{N}{L^3} \qquad (19)$$

Then, depending on salt concentration the solution can change from the semidilute to the dilute regime as c_s increases and the chain extension decreases. We will call c^*_s the salt concentration at which the polymer solution became dilute. In relation with the data presented in figure 4, we estimate that the systems become dilute at salt concentrations of $c^*_s \sim 1.66 \times 10^{-1}$ mM and $c^*_s \sim 1.66$ mM for P10 and at polymer concentrations of $c = 2.4 \times 10^{-1}$ mM and $c = 7.14 \times 10^{-1}$ mM respectively; for P20 at $c = 1.55 \times 10^{-1}$ and at $c = 2.4 \times 10^{-1}$ mM we find $c^*_s \sim 1.66$ mM and $c^*_s \sim 5 \times 10^{-1}$ mM respectively; for P25 at $c = 0.6 \times 10^{-4}$ mM, $c^*_s \sim 5 \times 10^{-2}$ mM and at $c = 1.55 \times 10^{-4}$ mM, $c^*_s \sim 1.66 \times 10^{-1}$ mM; finally, $c^*_s \sim 1.66$ mM for P50 at $c = 6.2 \times 10^{-4}$ mM. Now, from eqs 12 and 17, we obtain for the semidilute regime,

$$\frac{B}{c^{3/2}} \approx a_0(1+a_2c_s)^{-1/4} - a_1(1+a_2c_s)^{1/2}$$

$$a_0 = \frac{\Delta\alpha_m^0}{15(kT)^2}(1-\varphi)fe^2(NL)^{1/2}c^{-1/2}$$

$$a_1 = \frac{\Delta\alpha_m^0}{15(kT)^2}\varphi fe^2\frac{N}{L}c^{-1}$$

$$a_2 = \frac{2A}{c} \qquad (20)$$

For the dilute regime, we found from eqs 12 and 18

$$\frac{B}{c^{3/2}} \approx a_0(1+a_2c_s)^{-2/5} - a_1(1+a_2c_s)^{-1}$$

$$a_0 = \frac{\Delta\alpha_m^0}{15(kT)^2}(1-\varphi)fe^2(N^2L^4)^{1/5}c^{-2/5}$$

$$a_1 = \frac{\Delta\alpha_m^0}{15(kT)^2}\varphi fe^2\frac{N}{L}c^{-1}$$

$$a_2 = \frac{2A}{c} \qquad (21)$$

Let us first discuss the results in the dilute regime where c_s is high. If we suppose that at this high salt concentration $\Delta\alpha_m^0$ and φ do not change when more salt is added, we have $2Ac_s/c \gg 1$, and eq 21 reduces to:

$$\frac{B}{c^{3/2}} \approx a_0a_2{}^{-2/5}c_s{}^{-2/5} - \frac{a_1}{a_2}c_s{}^{-1} \qquad (22)$$

Equations 21 and 22 predict that B tends to zero at very high salt concentrations as seen experimentally (Figure 4). In Table 3 we report the fitting parameters obtained from experimental points and eq 22 and the calculated values of those parameters using the expressions for a_0, a_1, and a_2 in eq 21, Table 1 and the value of $\Delta\alpha_m^0$ obtained previously from

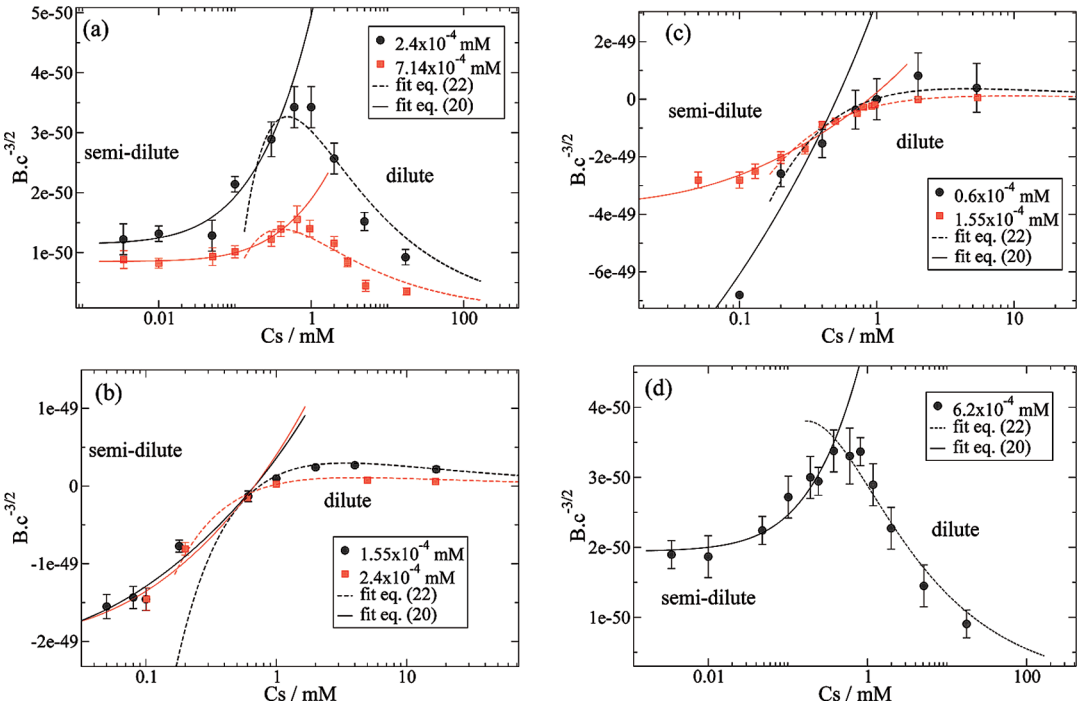

Figure 4. $B/c^{3/2}$ (in $mV^{-2}/(mol/m^3)^{3/2}$) as a function of salt concentration: (a) P10, (b) P20, (c) P25, and (d) P50. Lines are fittings using eq 20, 22.

eq 14 and Table 2. For these parameters, the fitting and calculated values are not far from each other; this is a bit surprising: first, the polarization distances of free and condensed counterions were taken as proportional to ξ and R respectively but not exactly equal and we expected a factor multiplying these distances and second, $\Delta\alpha_m^0$ and φ should be different from those of salt-free systems. Even more, we found values of a_2 which are in excellent agreement with the calculated ones (see Table 3). For example for P20 at a concentration $c = 1.55 \times 10^{-4}$ mM, we have $a_2 = 2A/c = 2 \times 5/4.43 \times 10^{23} = 2.91 \times 10^{-23}$ which is very close to the fitting value shown in Table 3, the same is true for the rest of the a_2 values of that table. The values of $(a_0 a_2^{-2/5})$ and (a_1/a_2) should be independent of polymer concentration and if we calculate the mean values for the two polymer concentrations of these quantities we found values which are in good accord with the calculated ones. For example, for P20 the average value for the two concentrations is $\langle a_0 a_2^{-2/5} \rangle = 1.7 \times 10^{-41}$ and the calculated one is 1.6×10^{-41}.

At low salt concentrations (semidilute solutions), $2Ac_s/c \ll 1$ and eq 20 becomes $Bc^{-3/2} = a_0 a_1 = cte$. In figure 4 we can see that B does not depend on salt concentration at very low ionic strength (see, for example, Figure 4a at $c_s < 0.1$ mM). The value of $Bc^{-3/2}$ is then the same as in salt-free systems: eq 20 reduces to eq 14 at $c_s = 0$. At higher salt concentrations, but still in the semidilute regime, the experimental points were fitted using eq 20 (see Figure 4). The fits are satisfactory and a_2 is close to $2A/c$. However, a_0 and a_1 differ from calculated values using eq 20, perhaps because in this range, $\Delta\alpha_m^0$ and φ could depend on salt concentration.

3.4. TEB Results. Polyelectrolyte−DTAB Solutions. Surfactants bearing a charge opposite to that of the polyelectrolyte are expected to replace the original counterions in the surroundings of the polyelectrolyte molecules and possibly eliminate the contribution of free counterions to the electrical birefringence. We have used here DTAB, known to form complexes when mixed with PAMPS.[23,24] The CACs of these systems are between 0.4 and 0.8 mM; at concentrations above 3 mM, the mixed systems become cloudy indicating incipient precipitation, hence we kept the surfactant concentration below this limit. The evolution of the Kerr constant as a function of DTAB concentration is shown on Figure 5. The inset in Figure 5a shows the evolution of the Kerr constant for pure DTAB solutions: B does not change up to a surfactant concentration of about 6 mM, which is far above the DTAB concentrations used in the PAMPS−DTAB mixed systems. Then the contribution of free DTAB molecules to the birefringence is negligible and all the changes found in B for the mixed systems should be attributed to the mixed complexes or to conformational changes of polymer molecules due to the presence of the surfactant. Figure 5a shows B as a function of DTAB concentration and, for comparison, with salt concentration, for P20 at $c = 2.6 \times 10^{-4}$ mM. The results are similar for others polyelectrolyte concentrations: figure 5b shows curves for P25 at different polyelectrolyte concentrations. P10 was not studied because it has not a clear CAC with DTAB due to its weak charge density.[11,23,25] We had not enough P50 to perform experiments with DTAB. However, figures 5a and b clearly demonstrate the difference between salts and surfactants. We see a change of the sign of the birefringence at a point which appears in the figure as a minimum (since we plot the absolute value of B). Equations 21 and 22 indicate that the birefringence tends continuously to zero as salt concentration increases. Below the concentration c_0 where B

Table 3. Fitting and Calculated Parameters from Eqs 22 and 21[a]

		$(a_0 a_2^{-2/5}) \times 10^{40}$		$(a_1/a_2) \times 10^{26}$		$(a_2 = 2A/c) \times 10^{23}$	
	c (mM)	fitting	calcd	fitting	calcd	fitting	calcd
P10	2.4×10^{-4}	1.33	0.122	0.646	0.540	3.51	3.32
	7.14×10^{-4}	0.532	0.122	0.234	0.540	1.92	1.1
P20	1.55×10^{-4}	2.53	1.60	4.19	1.64	2.98	2.91
	2.4×10^{-4}	0.90	1.60	1.72	1.64	2.01	1.89
P25	0.6×10^{-4}	5.99	1.26	1.06	1.24	6.40	6.41
	1.55×10^{-4}	1.0	1.26	3.37	1.24	2.59	2.46
P50	6.2×10^{-4}	1.14	1.78	0.373	0.612	0.54	0.54

[a] The parameters are expressed in MKS units: $\{a_0\} = m^5 \cdot V^{-2}$; $\{a_1\} = V^{-2} \cdot m^{-1}$; $\{a_2\} = m^3$.

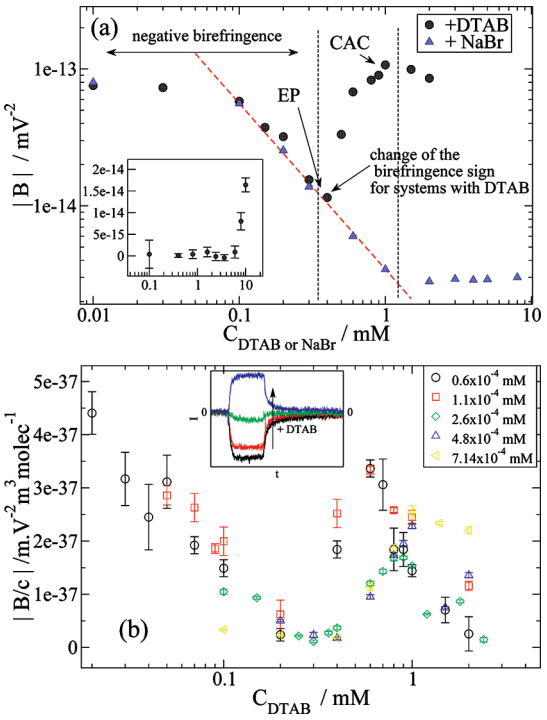

Figure 5. Kerr constant as a function of DTAB concentration. (a) P20 (109 mg·L^{-1})−DTAB system. Inset: Free-polyelectrolyte DTAB solution. (b) P25−DTAB. Inset: change of sign in the birefringence signals as DTAB increases.

changes sign, DTA^+ ions behave as a monovalent salt, the birefringence is identical to that of the samples with added NaBr (Figure 5a). This is because of the polarization and the *stationary* birefringence depends on the distribution of charges, it does not matter if they are bear by Na^+ or DTA^+. However a clear difference in behavior can be seen in the electric birefringence relaxation times results (future paper). This is no longer true for surfactants above c_0. The concentration c_0 is close to the point of equivalence of charges (EP), or isoelectric point, defined as the concentration of DTA^+ ions that equals the concentration of the polyelectrolyte Na^+ original counterions.[23] The CAC measured by techniques such as surface tension and potentiometry[23,24] is very close to the concentration corresponding to the maximum we can see in parts a and b of Figure 5. Between EP and CAC, the negative contribution to the birefringence is therefore suppressed by adding surfactant molecules. We have seen previously that this negative contribution corresponds to the polarization of free counterions in the direction perpendicular to the polyelectrolyte backbone. We conclude that DTA^+ ions replace the original polymer counterions, the surfactant ions come closer to the polyelectrolyte backbone than Na^+ (the original PAMPS counterion). This reduces the polarization in the direction perpendicular to the polymer main axis, lowers the negative contribution to the birefringence and as a result, B becomes positive: the polarization mechanism parallel to the polymer backbone dominates. At concentrations above the maximum, DTAB−PAMPS complexes start to form, which polarize less easily and the birefringence diminishes again (Figure 5b). Above a concentration of about 3 mM, precipitation begins and it is no longer possible to measure the birefringence due to the turbidity of the system. Let us comment the aggregation process. As DTA^+ ions replace Na^+ ones in the vicinity of the macromolecule backbone, the interaction between polymer molecules becomes less repulsive: water becomes progressively a bad solvent, hence the precipitation. This happens in the concentration range between the minimum ($B \sim 0$) and the maximum in the B vs surfactant concentration curves.

4. Conclusions

We presented experimental evidence on the counterion polarization mechanisms in flexible polyelectrolyte solutions. TEB results on polyelectrolyte solutions can be explained by assuming that free counterions polarize in the direction perpendicular to the main polymer axis and condensed counterions polarize parallel to it. We were able to demonstrate this by eliminating one of the two contributions to the birefringence produced by the polarization of counterions. By adding surfactant molecules which we know bind effectively to the polymer chain, close to the charged groups, we reduced the negative contribution, then eliminated it producing a change in the birefringence sign. We presented a simple model that explains the values of the Kerr constant for salt-free polyelectrolyte solutions as well as for salt/polyelectrolyte systems. This model permitted us to estimate the fraction of condensed counterions for each polyelectrolyte used. The results are in good agreement with the Manning prediction. The model also predicts a change in the sign of the birefringence as polyelectrolyte concentration increases which was considered an anomaly up to now.[9] This change is produced because as polymer concentration increases the negative contribution diminishes for the polymer used (PAMPS): at a certain concentration the positive contribution from condensed counterions dominates over the negative one which is produced by free counterions. Our work shows that TEB permits one to follow the aggregation process in polyelectrolyte/surfactant systems making it a very powerful technique for studying polyelectrolyte−surfactant complexation.

Acknowledgment. H.R. was partially supported by MEC under a Juan de la Cierva contract. We thank Jean François Argillier for the gift of polymer samples. The work was performed within the frame of a CNRS-CONICET cooperation program between France and Argentina (PICS 3175).

References and Notes

(1) Oosawa, F. *Polyelectrolytes*; Marcel Dekker. Inc.: New York, 1971.
(2) Imai, N.; Onishi, T. *Chem. Phys.* **1958**, *30*, 1115–1116.
(3) Oosawa, F. *J. Polym. Sci.* **1958**, *23*, 421–430.
(4) Manning, G. S. *J. Chem. Phys.* **1969**, *51*, 934–938. Manning, G. S. *J. Chem. Phys.* **1969**, *51*, 924–933. Manning, G. S. *Annu. Rev. Phys. Chem.* **1972**, *23*, 117–140.
(5) Oosawa, F. *Biopolymers* **1970**, *9*, 677–688. Minakata, A.; Imai, N.; Oosawa, F. *Biopolymers* **1972**, *11*, 347–359. Warashina, A.; Minakata, A. *J. Chem. Phys.* **1973**, *58*, 4743–4749. Mandel, M. *Mol. Phys.* **1961**, *4*, 489–496. Manning, G. S. *BioPhys. Chem.* **1978**, *9*, 65–70.
(6) Fixman, M. *Macromolecules* **1980**, *13*, 711–716. Fixman, M.; Jagavmathan, S. *J. Chem. Phys.* **1981**, *75*, 4048–4059.
(7) Bordi, F.; Cametti, C.; Colby, R. H. *J. Phys. Condens. Matter* **2004**, *16*, R1423–R1463.
(8) Ookubo, N.; Hirai, Y.; Ito, K.; Hayakawa, R. *Macromolecules* **1989**, *22*, 1359–1366. Ito, K.; Yagi, A.; Ookubo, N.; Hayakawa, R. *Macromolecules* **1990**, *23*, 857–862. Nagamine, Y.; Ito, K.; Hayakawa, R. *Langmuir* **1999**, *15*, 4135–4138.
(9) Kramer, U.; Hoffmann, H. *Macromolecules* **1991**, *24*, 256–263. Cates, M. E. *J. Phys. II*, (*Fr.*) **1992**, *2*, 1109–1119.Schlagberger, X.; Netz, R. R. *EPL*, **2008**, *83*, 36003, p 1−p 6.Washizu, H.; Kikuchi, K. *J. Phys. Chem. B* **2002**, *106*, 11329–11342.Kang, K; Dhont, J. K. G. *EPL*, **2008**, *84*, 14005, p 1−p 6.
(10) Goddard, E. D.; Ananthapadmanabhan, K. P. *Interaction of Surfactants With Polymers and Proteins*; CRC Press: Boca Raton, FL, 1993. Kwak, J. C. T. *Polymer-Surfactant Systems*; Marcel Dekker: New York, 1998.
(11) Ritacco, H.; Kurlat, D. H. *Colloids Surf. A* **2003**, *218*, 27–45.

(12) de Gennes, P.-G.; Pincus, P.; Velasco, R. M.; Brochard, F. *J. Phys.* (*Paris*) **1976**, *37* (12), 1461–1473.
(13) Odijk, T. *J. Polym. Phys., Part B* **1977**, *15*, 477–483. Skolnick, J.; Fixman, M. *Macromolecules* **1977**, *10*, 944–948. Barrat, J. L.; Joanny, J. F. *Adv. Chem. Phys*. **1996**, *XCIV*, 1.
(14) Odijk, T. *Macromolecules* **1972**, *12*, 658–693.
(15) Khokhlov, A. R.; Khachaturian, K. A. *Polymer* **1982**, *23*, 1793–1802.
(16) Manghi, M.; Netz, R. R. *Eur. Phys. J.* **2004**, *14*, 67–77.
(17) de Gennes, P.-G. *Scaling Concepts in Polymer Physics*; Cornell University Press: London, 1979.
(18) Frederic, E.; Houssier, C. *Electric Dichroism and Electric Birefringence*; Clarendon Press: Oxford, U.K., 1973.
(19) Ariel, G.; Andelman, D. *Europhys. Lett*. **2003**, *61* (1), 67–73.
(20) Lachenmayer, K.; Oppermann, W. *J. Chem. Phys*. **2002**, *116*, 392–398.
(21) Johner, C.; Kramer, H.; Martin, C.; Biegel, J.; Deike, R.; Weber, R. *J. Phys. II* (*Fr*.) **1995**, *5*, 721–732.
(22) Dobrynin, A. V.; Colby, R. H.; Rubinstein, M. *Macromolecules* **1995**, *28*, 1859–1871.
(23) Ritacco, H.; Kurlat, D.; Langevin, D. *J. Phys. Chem. B* **2003**, *107*, 9146–9158.
(24) Jain, N.; Trabelsi, S.; Guillot, S.; McLoughlin, D.; Langevin, D.; Letellier, P.; Turmine, M. *Langmuir* **2004**, *20*, 8496–8503.
(25) Ritacco, H.; Acosta, E.; Bisceglia, M.; Kurlat, D. *Phys. Chem. Liq*. **2002**, *40*, 491–505.